THE SOLAR PROMINENCES MAGNETIC FIELD MEASUREMENTS

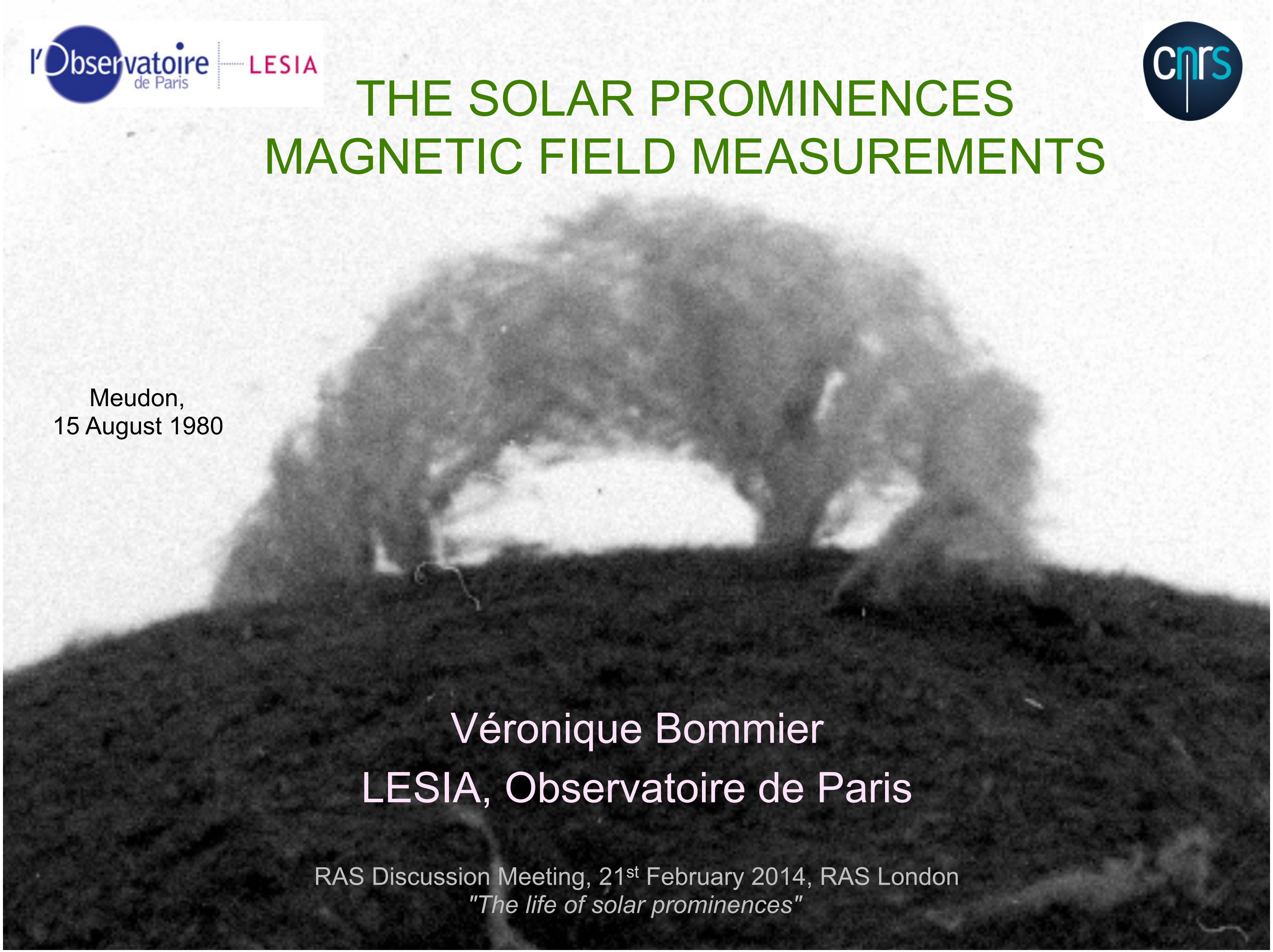

Meudon,
15 August 1980

Véronique Bommier
LESIA, Observatoire de Paris

RAS Discussion Meeting, 21st February 2014, RAS London
"The life of solar prominences"

1st GENERATION HANLE EFFECT OBSERVATIONS

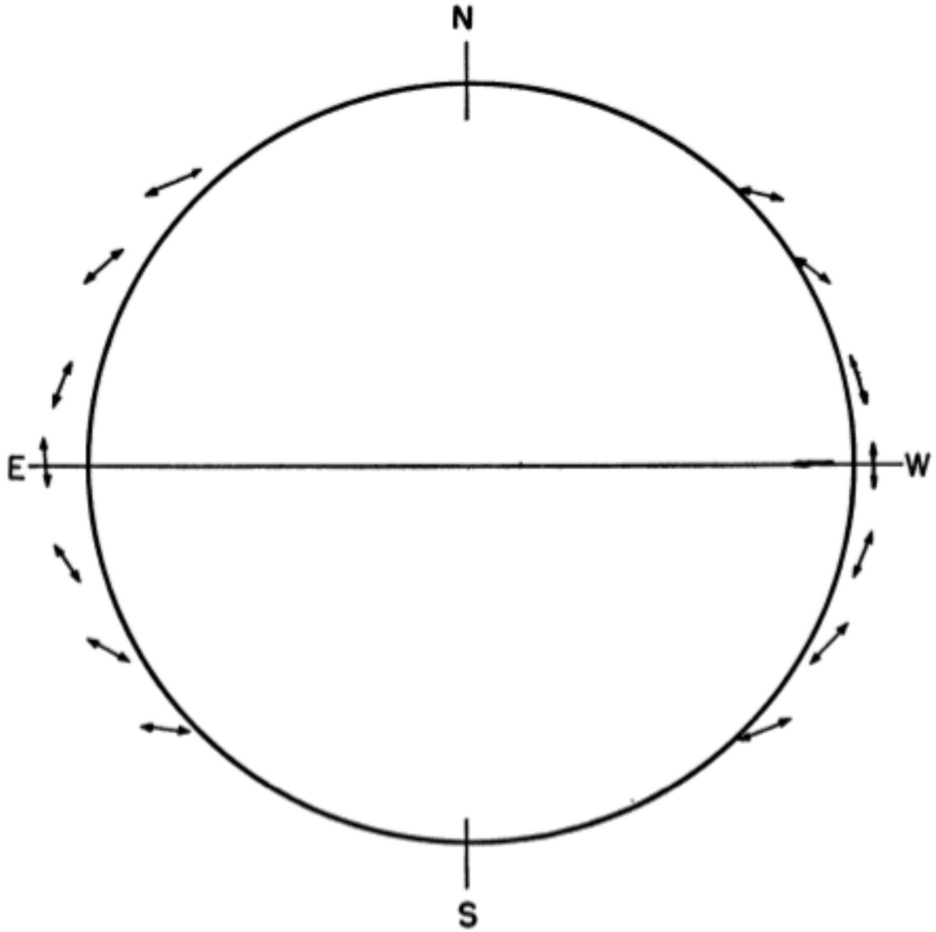

FIG. 1.—Directions of polarization observed by Lyot in Hα and in D_3 in 1932 and in 1935

Hyder, C., 1965, Ap., 141, 1374

1st GENERATION HANLE EFFECT OBSERVATIONS

interpretation in terms of the Hanle effect

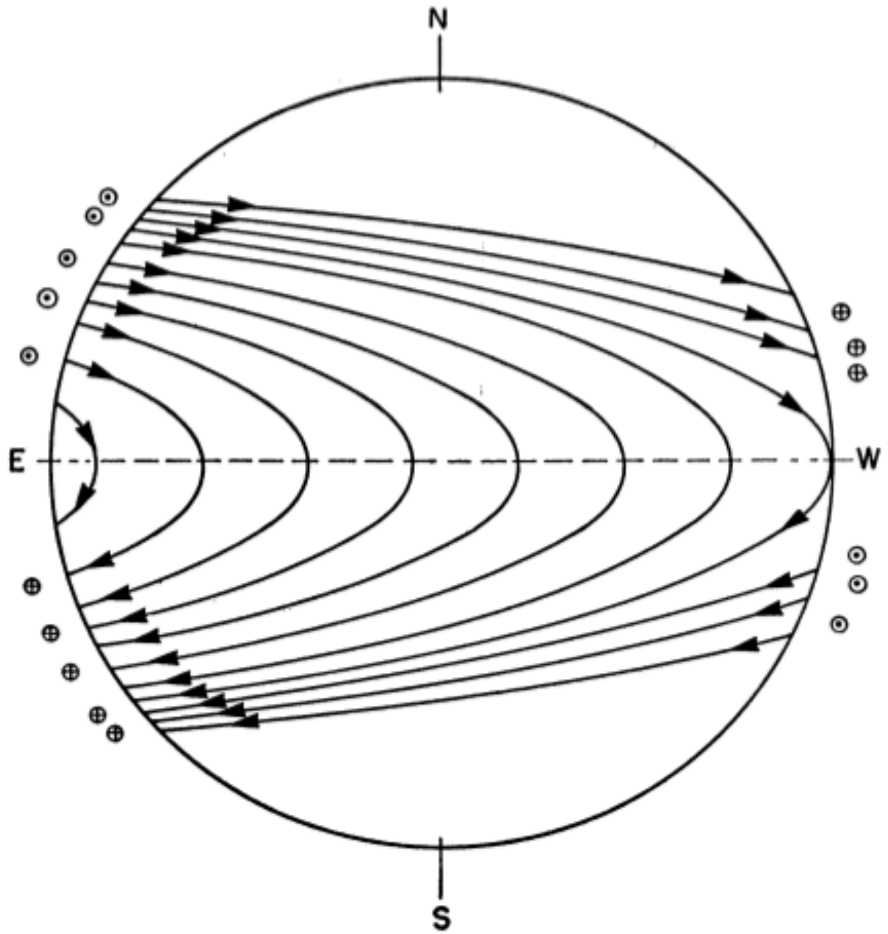

FIG. 2.—Model for the directions of prominence magnetic fields as a function of solar latitude and longitude for Lyot's prominences. The directions of the fields at the limb are toward (*circle with dot*) and away from (*circle with cross*) the observer.

Hyder, C., 1965, Ap., 141, 1374

2nd GENERATION HANLE EFFECT OBSERVATIONS

Observations at the Pic-du-Midi coronagraph:
- project: the whole cycle XXI
- accuracy: 10 times better (2 digits)
- quiescent prominences

quiescent prominence observed on 19 December 1975 (beginning of the program)

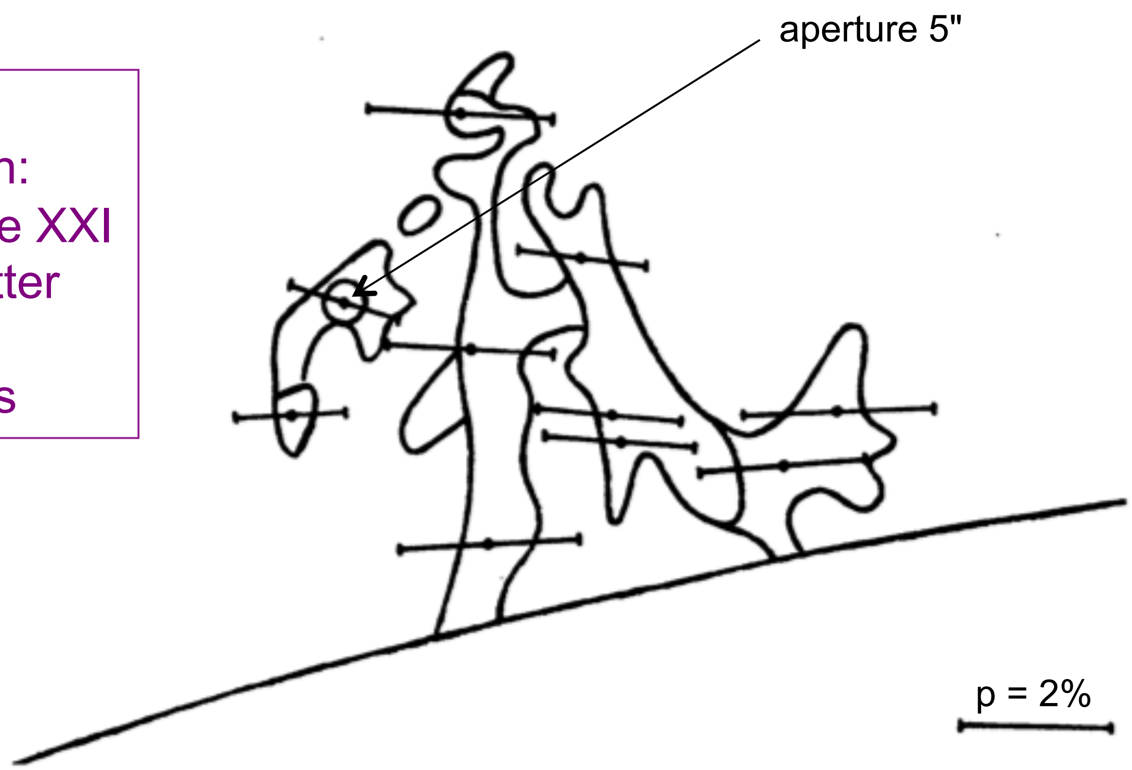

Fig. 1. The distribution of D 3 line polarization over the apparent surface of a quiescent prominence (19.12.1975). The bar in the lower right corner corresponds to a degree of polarization, $p=0.020$ and the field aperture is 5″ wide

Leroy, Ratier, Bommier, 1977, A&A, 54, 811

THEORY OF THE HANLE EFFECT

Coherences:
off-diagonal elements
of the atomic density matrix

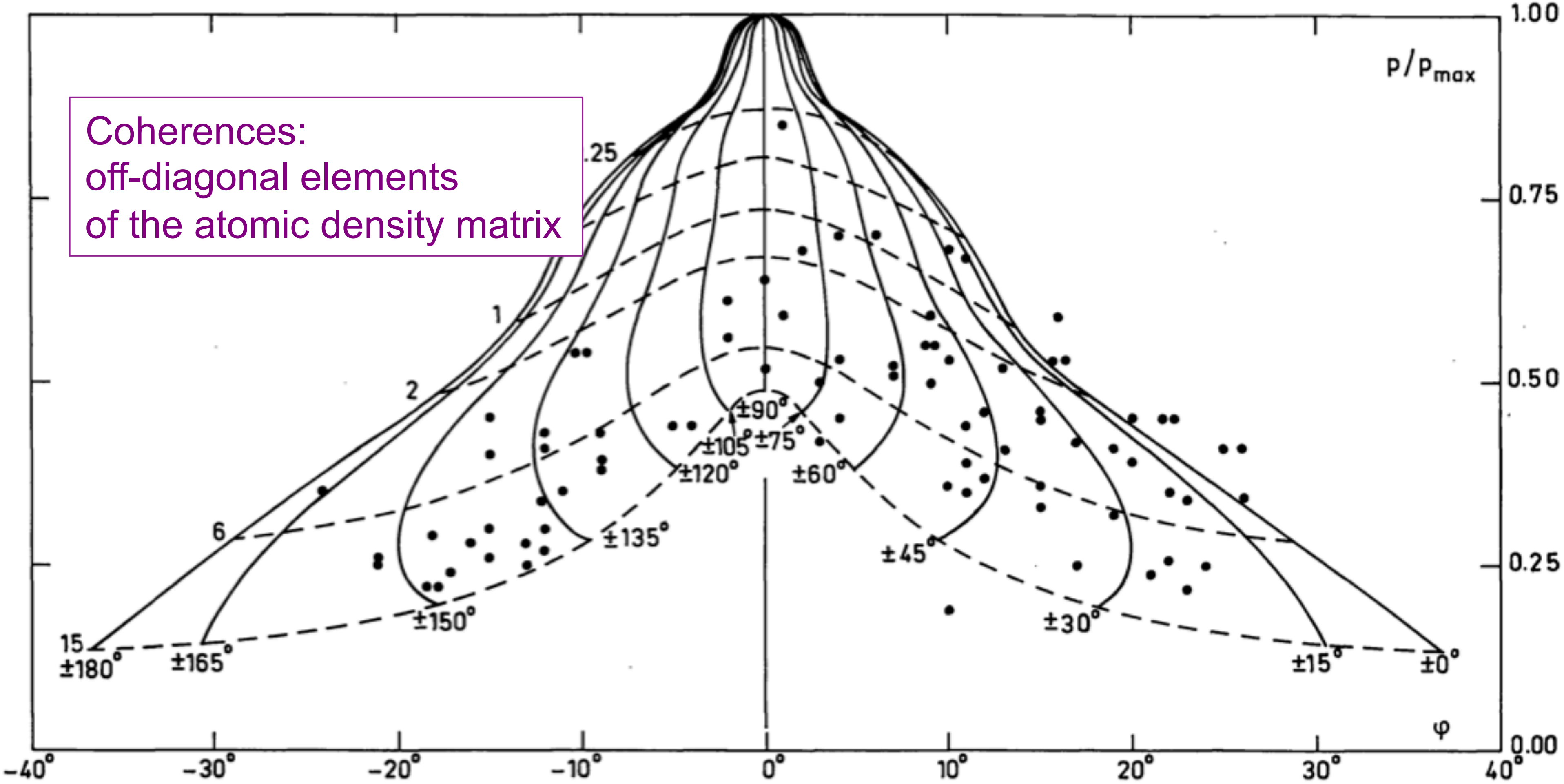

Sahal-Bréchot, Bommier, Leroy, 1977, A&A, 59, 223

THE HANLE EFFECT

a non-linear and anisotropic effect

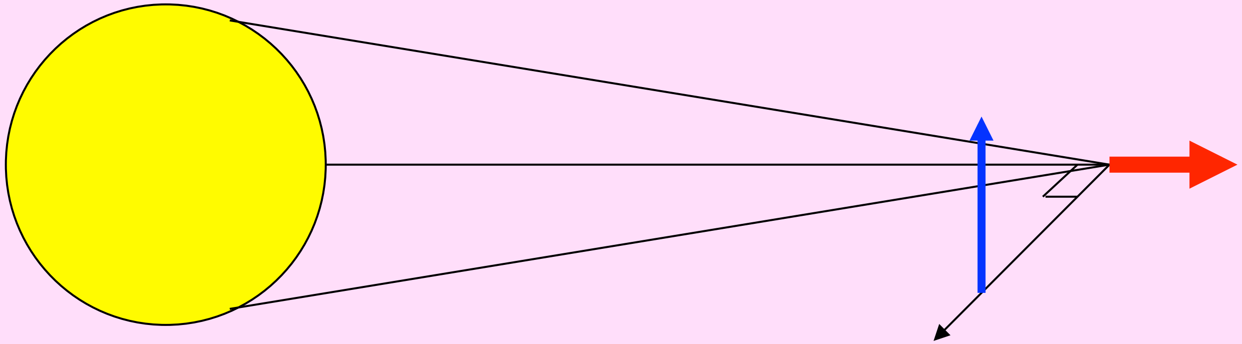

• vertical field:
=> no effect

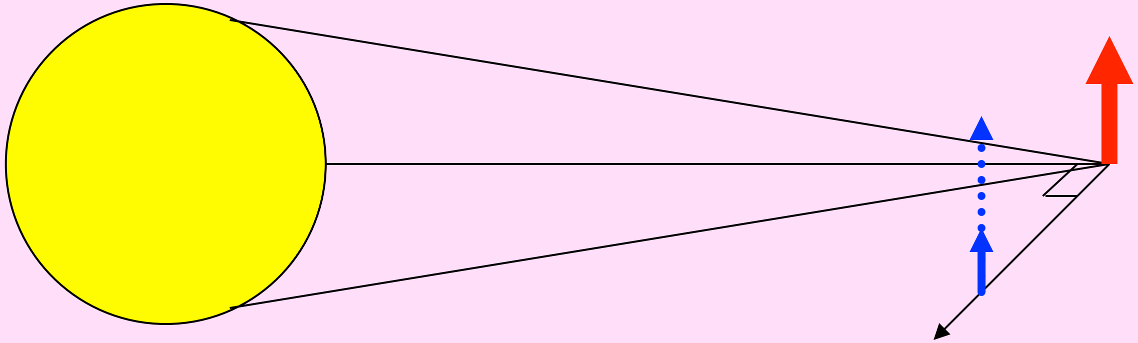

• meridian field:
=> depolarisation

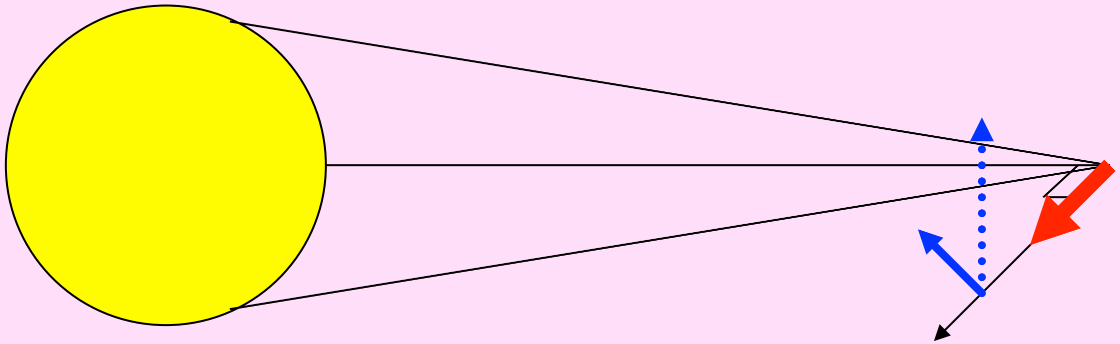

• parallel (toroidal) field:
=> depolarisation
+ rotation of the
polarisation durection

ARE ZEEMAN & HANLE EFFECTS COMPLEMENTARY ?

not really:

same strengths
and
same weaknesses

at limb:

the vertical field
(Hanle insensitive)
is the transverse field
for the Zeeman effect

this would be different
at disk center

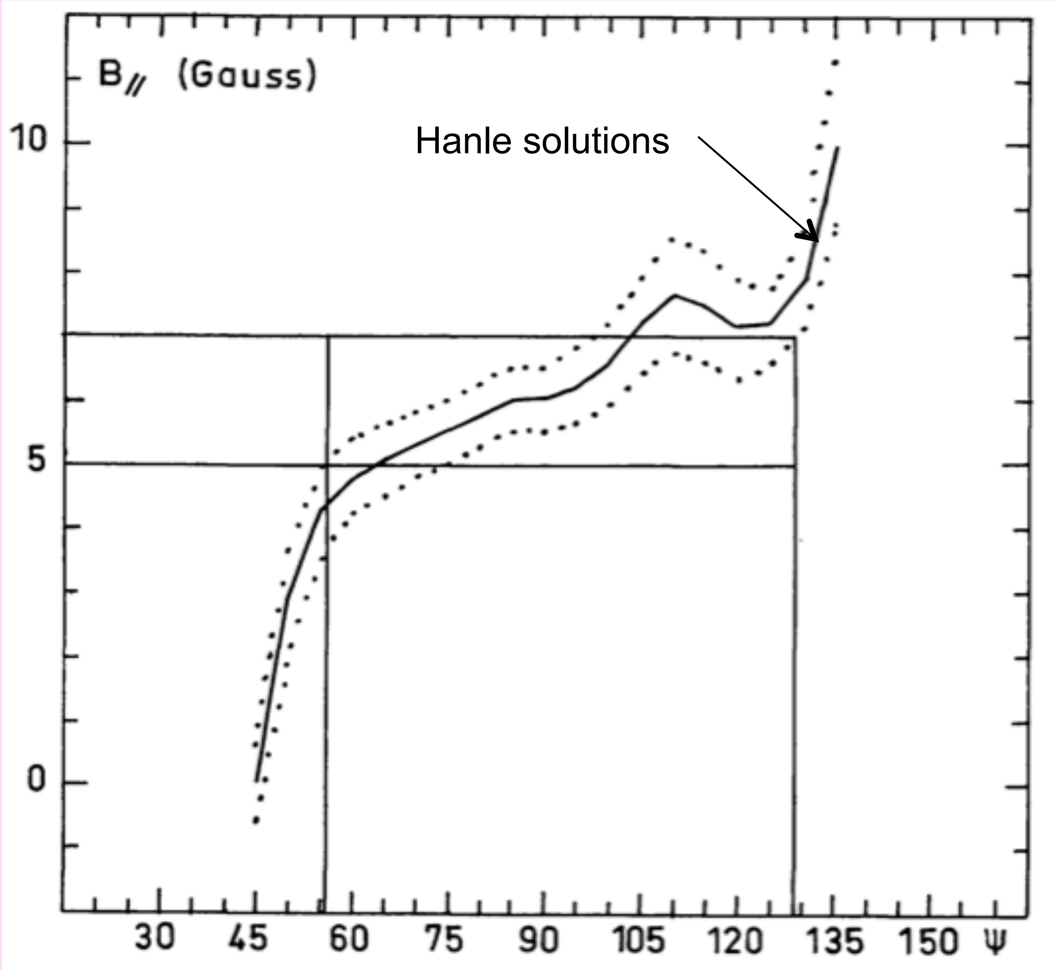

Bommier, Sahal-Bréchot, Leroy, 1981, A&A, 100, 231

FIRST EVIDENCE OF THE HORIZONTAL FIELD

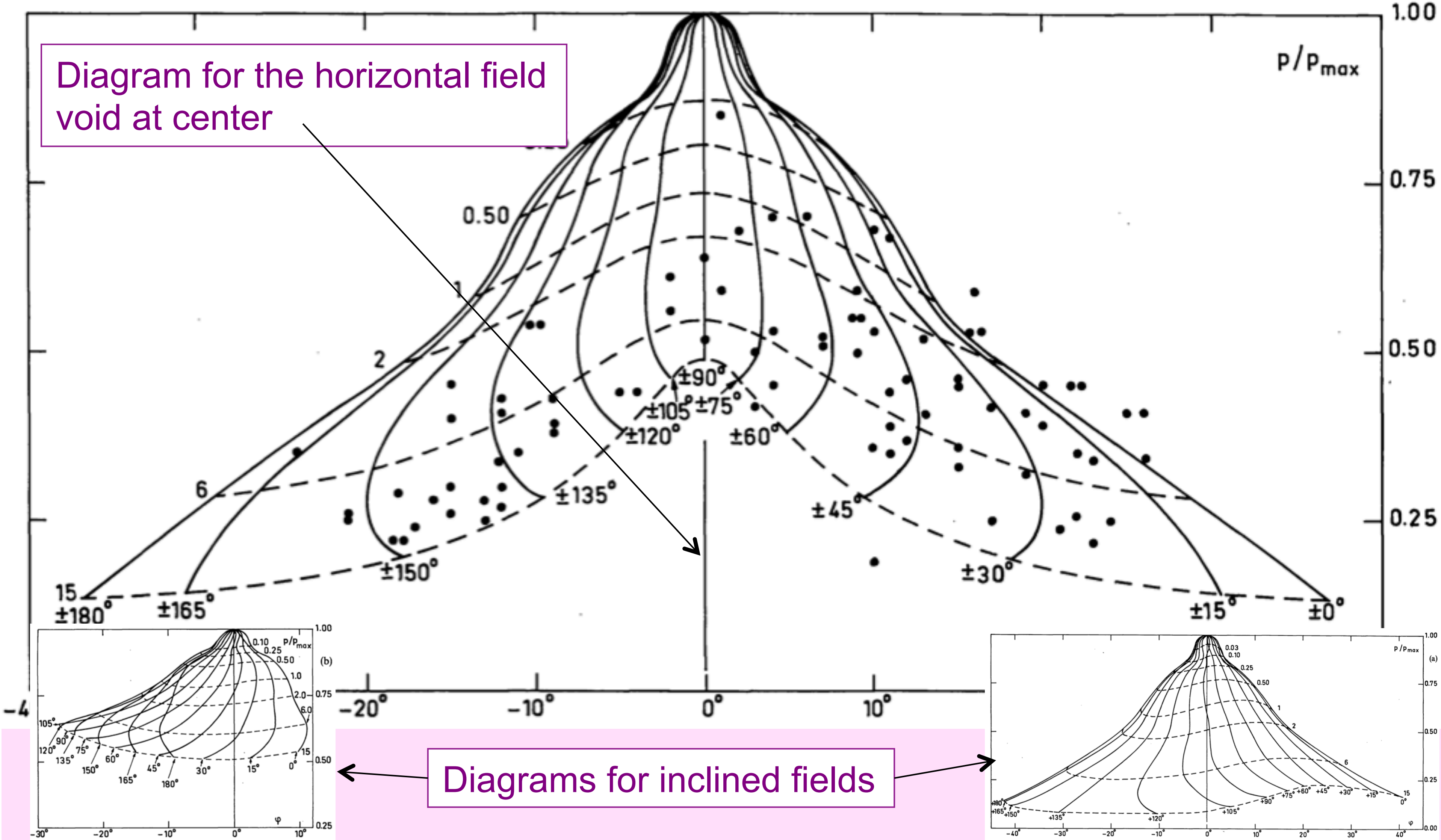

Sahal-Bréchot, Bommier, Leroy, 1977, A&A, 59, 223 inclination angle

SECOND EVIDENCE OF THE HORIZONTAL FIELD

Date and location	Obs. no.	χ	h	B	θ	ϕ	ϕ^*_r, ϕ^*_s
15 August, 1980	1.2 *D*	– 18	65	17	78	90	60, – 120
PA 121	2.2 *D*	– 18	70	10	90	108	78, – 138
AA 30	3.3 *D*	– 18	80	12 (14)	84 (85)	62 (108)	78, – 138
	4.2 *D*	– 18	55	20 (21)	78 (80)	56 (105)	75, – 135
	5.2 *D*	– 18	70	17 (15)	90 (85)	108 (107)	78, – 138
	6.2 *D*	– 18	85	25 (25)	84 (85)	114 (115)	85, – 145
	7.2 *D*	– 18	95	15 (14)	90 (85)	114 (113)	83, – 143
	8.2 *D*	– 18	55	25 (26)	84 (85)	108 (106)	77, – 137
	9.2 *D*	– 18	60	17 (16)	90 (85)	114 (106)	80, – 140
	10.2 *D*	– 18	75	25 (22)	84 (85)	66 (112)	82, – 142
	11.2 *D*	– 18	85	15 (14)	84 (85)	102 (105)	74, – 134
	12.2 *D*	– 18	95	25 (13)	72 (85)	108 (116)	82, – 142
	13.2 *D*	– 15	45	27 (15)	78 (85)	102 (94)	68, – 128
	14.2 *D*	– 15	55	20 (16)	90 (85)	114 (104)	79, – 139
	15.2 *D*	– 15	65	15 (21)	84 (85)	102 (107)	75, – 135
	16.2 *D*	– 15	80	22 (22)	84 (85)	114 (115)	85, – 145
	17.2 *D*	– 15	90	27 (26)	84 (85)	72 (100)	70, – 130
	18.2 *D*	– 15	95	30 (21)	78 (90)	108 (118)	83, – 143
	19.2 *D*	– 15	105	17 (21)	90 (90)	120 (125)	93, – 153
	20.2 *D*	– 12	35	22 (24)	84 (85)	144 (141)	112, – 172

2-line observations:
the 2 components
of He I D3
Stokes II @ SacPeak

Athay, Querfeld, Smartt, Landi Degl'Innocenti, Bommier, 1983, Solar Phys., 89, 3

CONFIRMATION OF THE HORIZONTAL FIELD

2-line observations:
He I D3 + Hβ
at Pic-du-Midi

field dip model

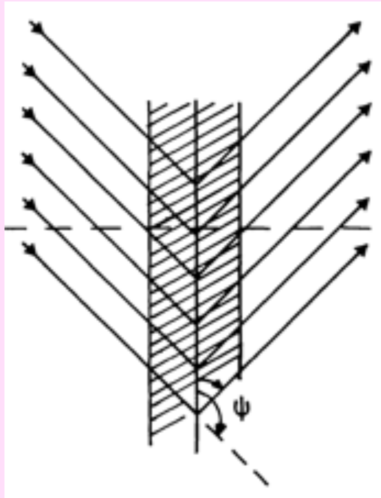

No.	ψ, $180° - \psi$ (deg)	θ (deg)	α (deg)	B Gauss	N_e 10^{10} cm^{-3}
4A	75,105	35	25	16	4
4B	90,90	20	10	14	1.5
4C	70,110	30	20	12	0.7
6	50,130	65	35	6	1
7	60,120	− 70	0	8	3
8N	65,115	− 55	35	5	4
8S	45,135	−120	40	4	0.7
9	60,120	− 95	15	5	0.7
10	45,135	25	15	10	0.3
11	70,110	− 45	35	7	1
12	90,90	30	10	11	0.1
13	85,95	− 65	75	2	0.5
14	90,90	35	25	12	0.3
15	90,90	125	5	14	1

Bommier, Sahal-Bréchot, Leroy, 1986, A&A, 156, 79

2-line observations:
He I D3 + Hβ
at Pic-du-Midi

+ THE ELECTRON DENSITY

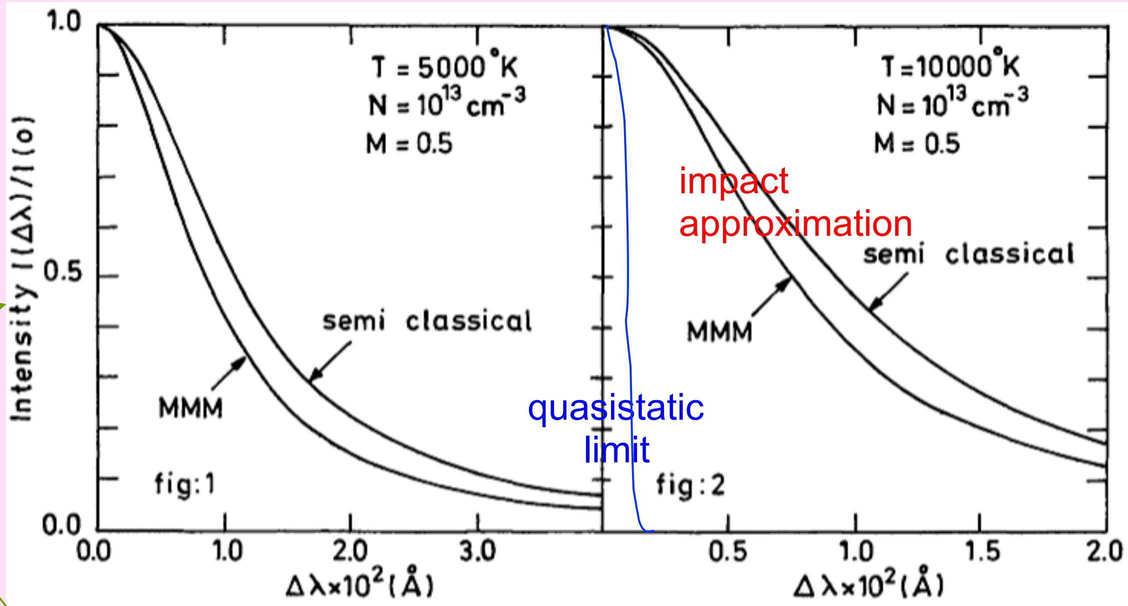

Stehlé, Mazure, Nollez, Feautrier, 1983, A&A 127, 263

N_e 10^{10} cm^{-3}
4
1.5
0.7
1
3
4
0.7
0.7
0.3
1
0.1
0.5
0.3
1

From eclipse observations and emission measure,
Jejcic, Heinzel et al. obtain similar densities $5 \times 10^9 < N_e < 10^{11}$ cm^{-3}
Jejcic, Heinzel, Zapior, Druckmüller, Gunar, Kotrc, 2013, IAUS300, 420

Bommier, Leroy, Sahal-Bréchot, 1986, A&A, 156, 90

THE AMBIGUITY DILEMMA

Normal or
Inverse
Polarity ?

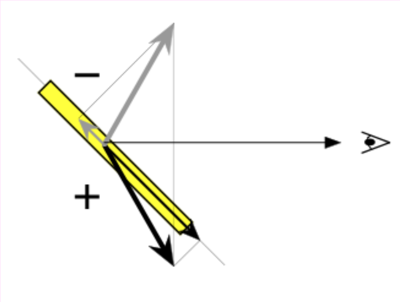

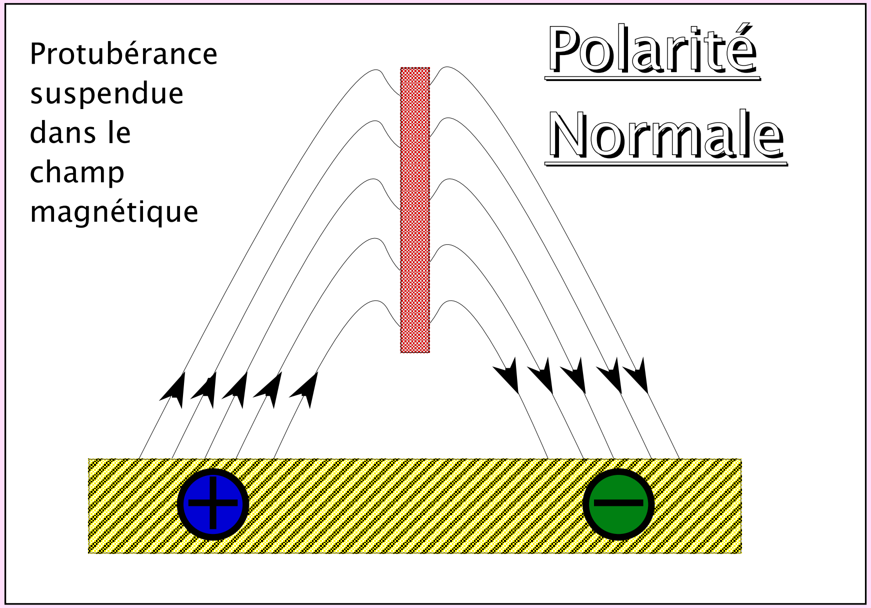

Kippenhahn & Schlüter-type model:
Normal Polarity

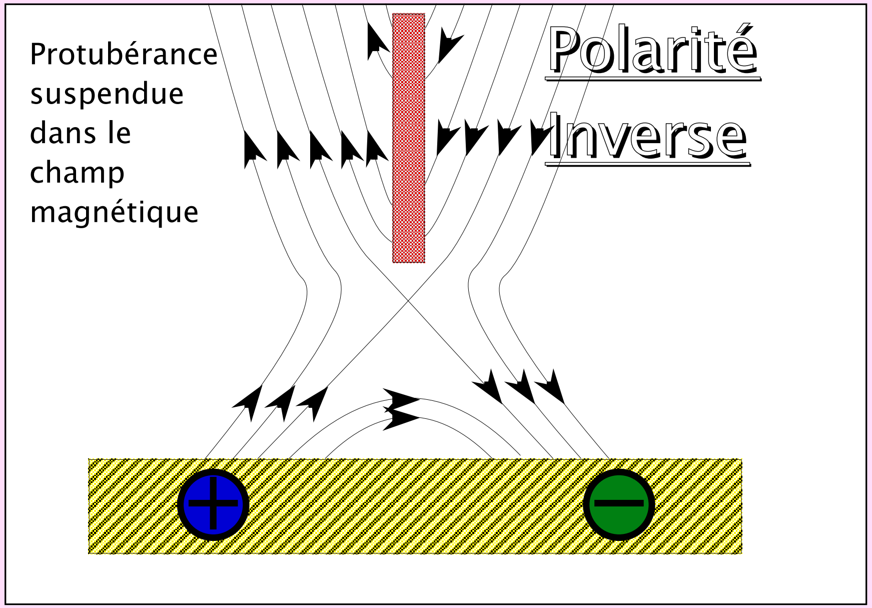

Kuperus & Raadu-type model:
Inverse Polarity

THE POLAR CROWN PROMINENCES

vertical gradient
+ 0.5 G/10,000 km

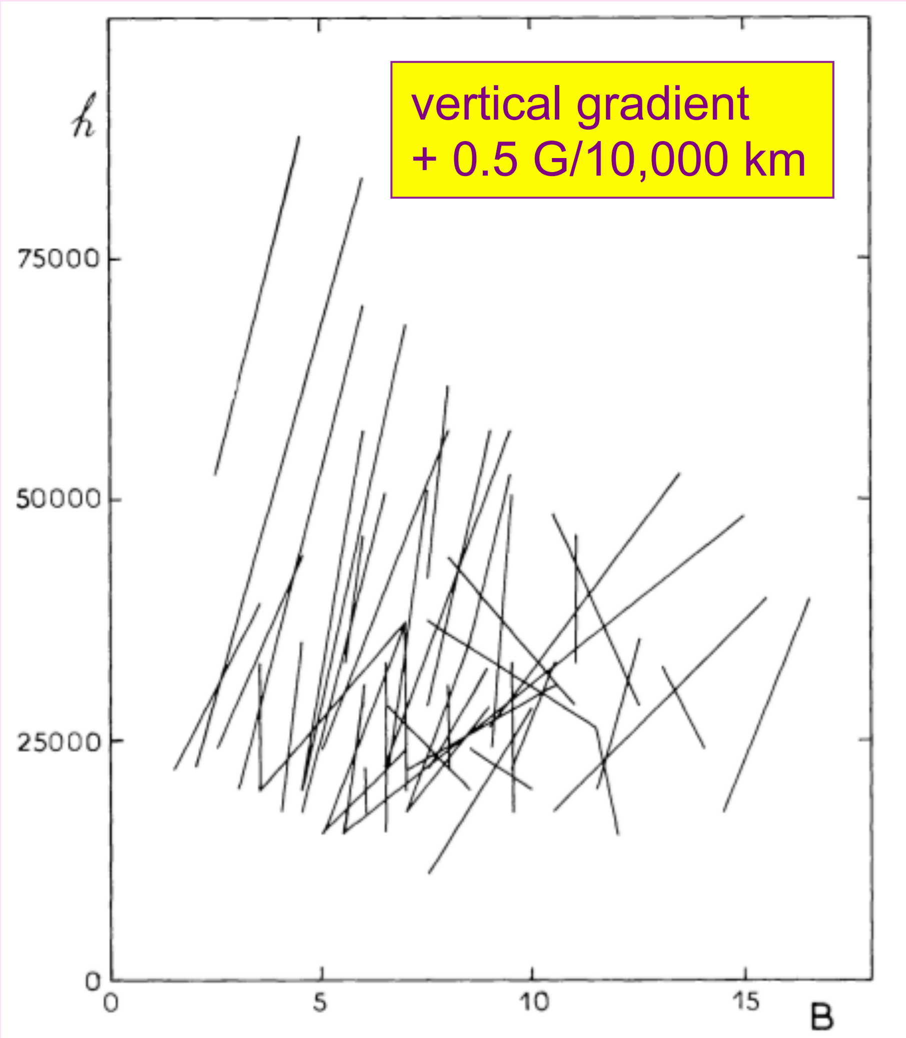

first evidence
of a global organization

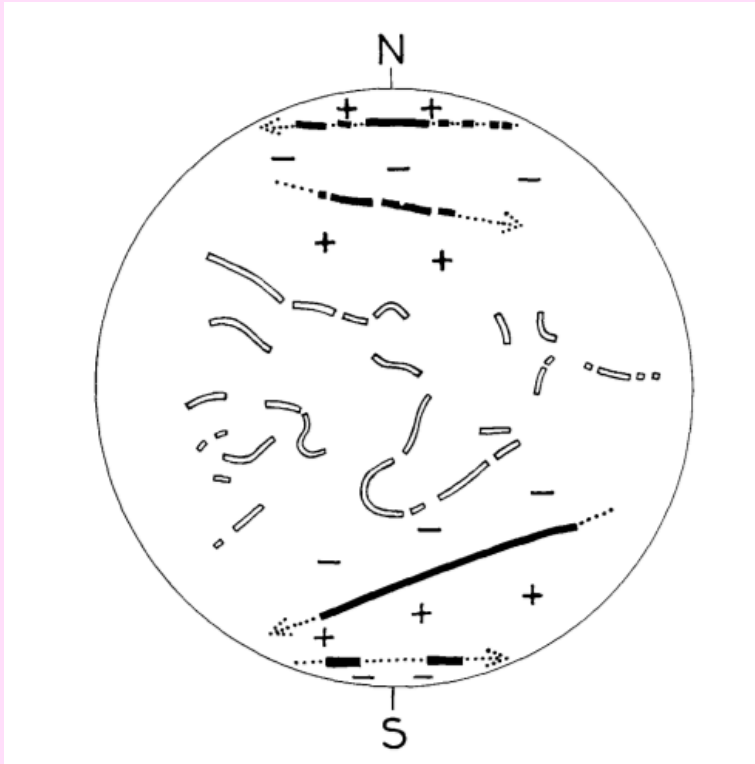

Leroy, Bommier, Sahal-Bréchot, 1983, Solar Phys., 83, 135

1st AMBIGUITY RESOLUTION

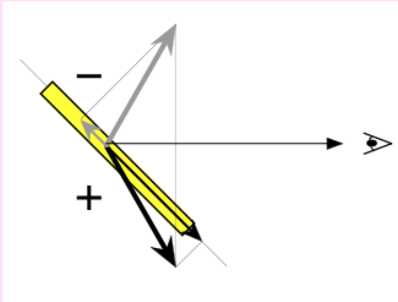

– the symmetry depends on the scattering angle:
  - rigorous l.o.s. symmetry at 90° scattering (exact limb)
  - different symmetry elsewhere

– **comparing 2 following days observations** permits to eliminate the ghost solution, that changes under solar rotation

– our result on 20 prominences: a large majority of **Inverse Polarity Prominences** (1980)

Bommier, Sahal-Bréchot, Leroy, 1981, A&A, 100, 231

2nd AMBIGUITY RESOLUTION

satistical analysis
of the mirror effect
of the ghost solution,
assuming a constant
α angle

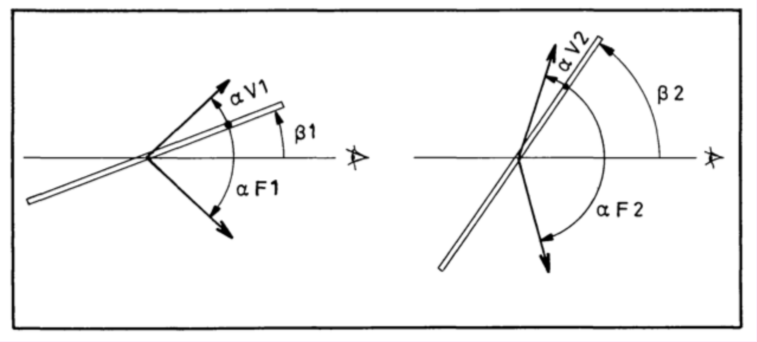

– sample of 256 prominences
(medium and low latitude)

– h < 30,000 km and sharp-edged
large majority of Normal Polarity

– h > 30,000 km, filamentary or curtain-like
large majority of Inverse Polarity

– small angle (25°) between the field
and the prominence long axis

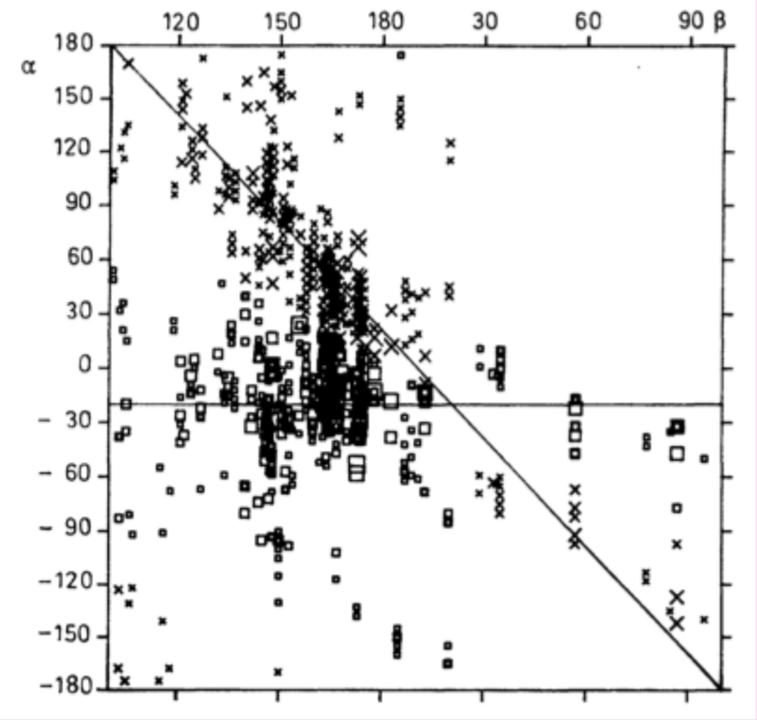

Leroy, Bommier, Sahal-Bréchot, 1984, A&A, 131, 33

CYCLIC EVOLUTION

OF THE

GENERAL ORGANIZATION

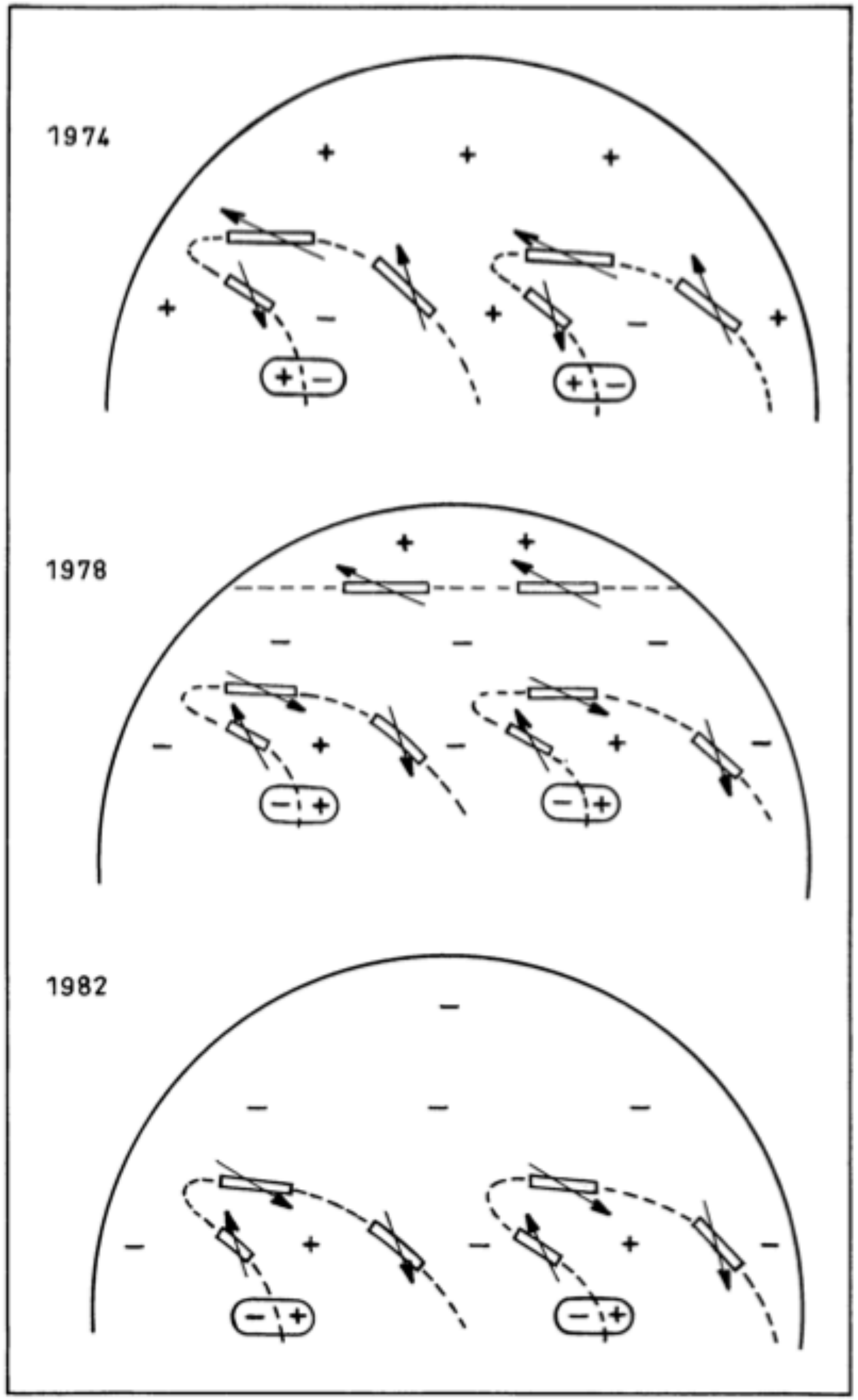

Leroy, Bommier, Sahal-Bréchot, 1984, A&A, 131, 33

3rd AMBIGUITY RESOLUTION

optical thickness effect:

comparison of
an optically thin (He I D3) and
an optically thick line (Hα)

the scattering geometry
is different
(internal radiation and absorption
for the optically thick line)

=> the symmetry of the solutions
is different

elimination of the **ghost solution**

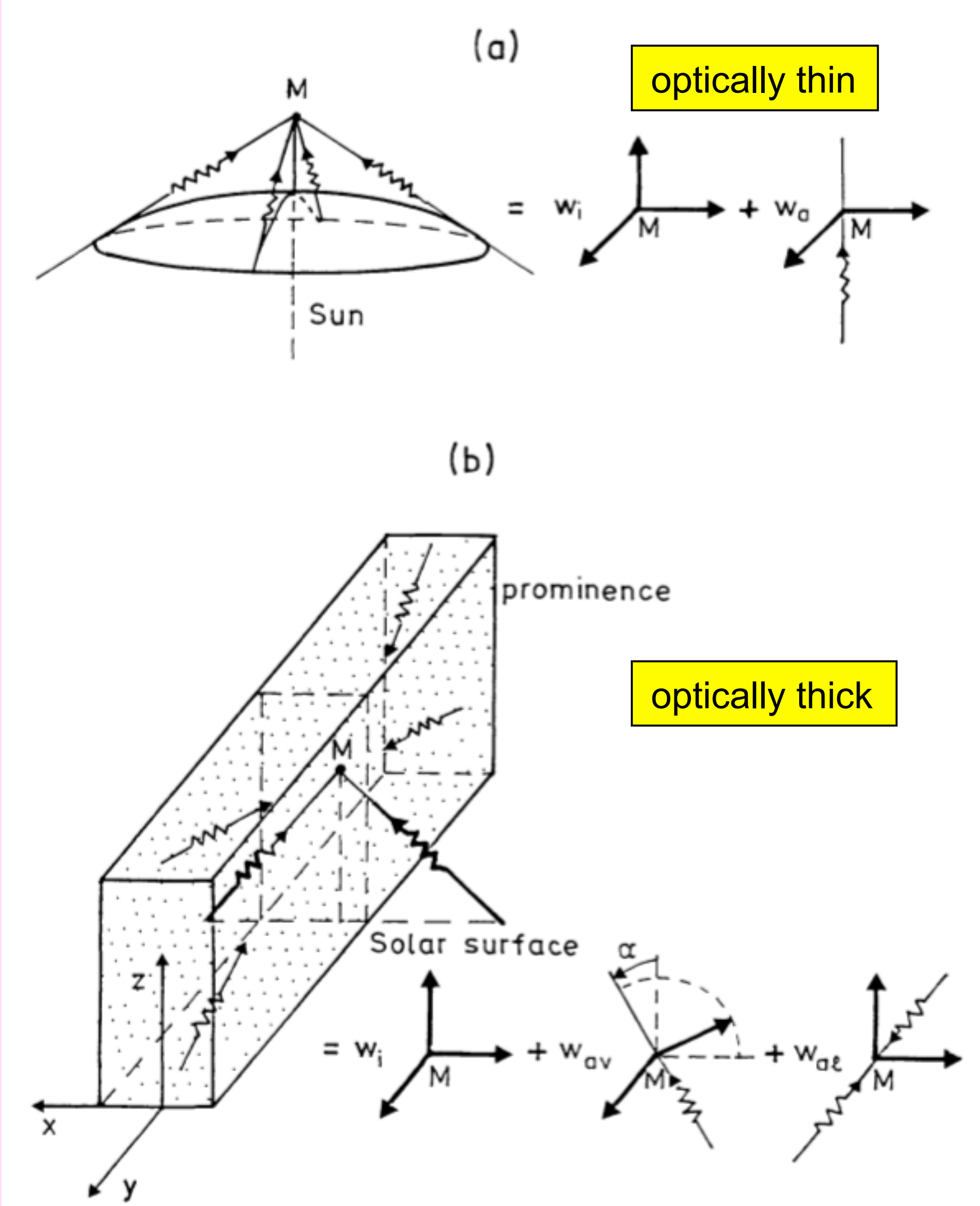

Landi Degl'Innocenti, Bommier,
Sahal-Bréchot, 1987, A&A, 186, 335

Bommier, Landi Degl' Innocenti, Leroy, Sahal-Bréchot, 1994, Solar Phys., 154, 231

			magnetic field vector and electron density (true solution)					magnetic field vector and electron density (symmetrical solution)				
Pr.	#op.	date	B	θ (D3)	θ (Hα)	ψ	Ne cm-3	B	θ (D3)	θ (Hα)	ψ	Ne cm-3
INVERSE PROMINENCES												
#1	#-19	15/5/79	6.68	-60.7	-59.4	45	2.60E+10	3.99	43.8	17.0	45	3.30E+10
#2	#-21	21/6/79	3.28	-70.2	-84.4	45	1.70E+10	5.38	82.2	56.8	45	2.10E+10
#2	#-22	22/6/79	5.29	-79.8	-101.7	60	7.50E+09	3.45	77.3	48.0	60	1.10E+10
#3	#-23	5/7/79	4.80	-78.6	-92.5	60	1.90E+10	6.89	78.3	57.5	60	2.20E+10
#3	#-24	6/7/79	6.17	-63.5	-64.2	75	3.20E+09	3.73	47.0	22.1	75	9.00E+09
#4	#+25	6/7/79	2.34	-117.0	-111.5	45	7.50E+09	3.62	107.5	122.2	45	7.50E+09
#5	#-28	21/6/80	7.88	-83.8	-63.7	90	2.70E+10	12.15	96.2	56.5	90	2.30E+10
#6	#-32	18/7/80	5.64	-103.7	-74.1	45	5.30E+10	8.17	121.7	77.5	45	5.30E+10
#6	#-33	19/7/80	8.59	-99.2	-53.9	45	3.70E+10	10.00	115.8	53.1	45	3.90E+10
#7	#-70	21/7/80	15.10	-48.5	-48.2	75	8.80E+09	9.43	54.4	39.7	75	1.90E+10
#9	#-88	29/6/80	8.15	-94.2	-87.6	60	2.50E+09	6.06	94.0	70.6	60	2.70E+09
#10	#+89	29/6/80	6.97	-114.3	-120.3	90	1.40E+10	8.71	118.1	131.4	90	1.10E+10
#12	#+127	21/6/79	7.96	-99.7	-99.6	60	6.30E+10	8.93	89.1	116.2	60	6.80E+10
#13	#-256	6/7/79	9.88	30.5	13.4	90	7.80E+09	9.33	-41.7	-15.4	90	1.00E+10
#14	#-261	1/8/79	13.41	29.7	48.8	45	2.70E+10	8.93	-59.8	-33.1	45	3.90E+10
#14	#-262	2/8/79	8.35	48.0	48.8	45	2.00E+10	9.45	-62.3	-43.0	45	2.20E+10
		average values	7.53			61	2.13E+10	7.39			61	2.44E+10
		standard deviations	3.30			18		2.70			18	
		average values (log.)					1.50E+10					1.84E+10
		min	2.34			45	2.50E+09	3.45			45	2.70E+09
		max	15.10			90	6.30E+10	12.15			90	6.80E+10
NORMAL PROMINENCES												
#8	#+80	17/7/80	13.41	-150.3	-156.5	90	6.40E+09					
#11	#-124	23/6/79	12.93	36.4	10.8	90	1.10E+10	5.70	·17.9		90	
		average values	13.17			90	8.70E+09	5.70			90	
		standard deviations	0.34			0						
		average values (log.)					8.39E+09					

FINAL SYNOPTIC MAPS

Ambiguity resolution:

Inverse & Longitudinal methods

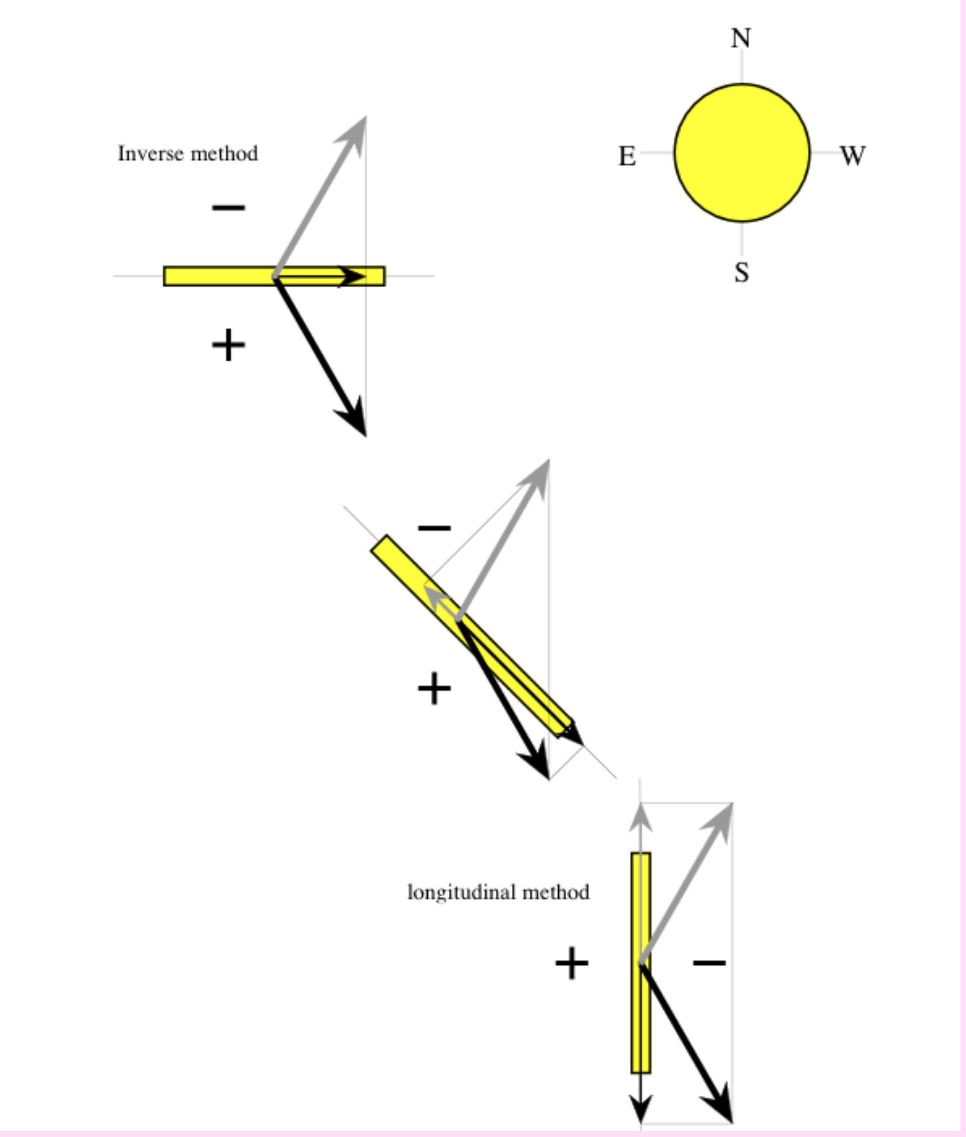

323 prominences observed in 1974-1982, ascending phase of cycle XXI

24 synoptic maps, one example:

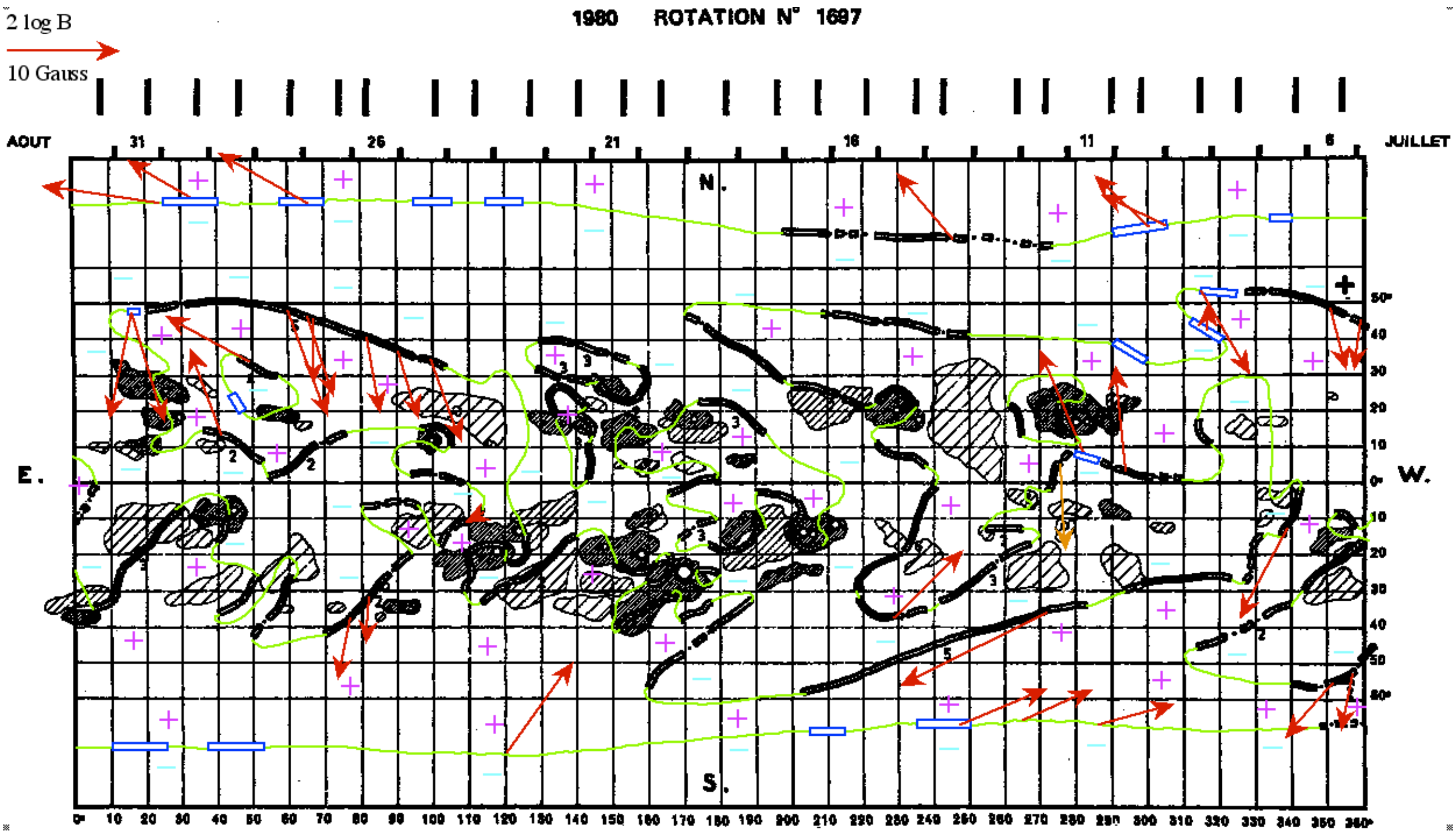

CYCLIC EVOLUTION

OF THE

GENERAL ORGANIZATION

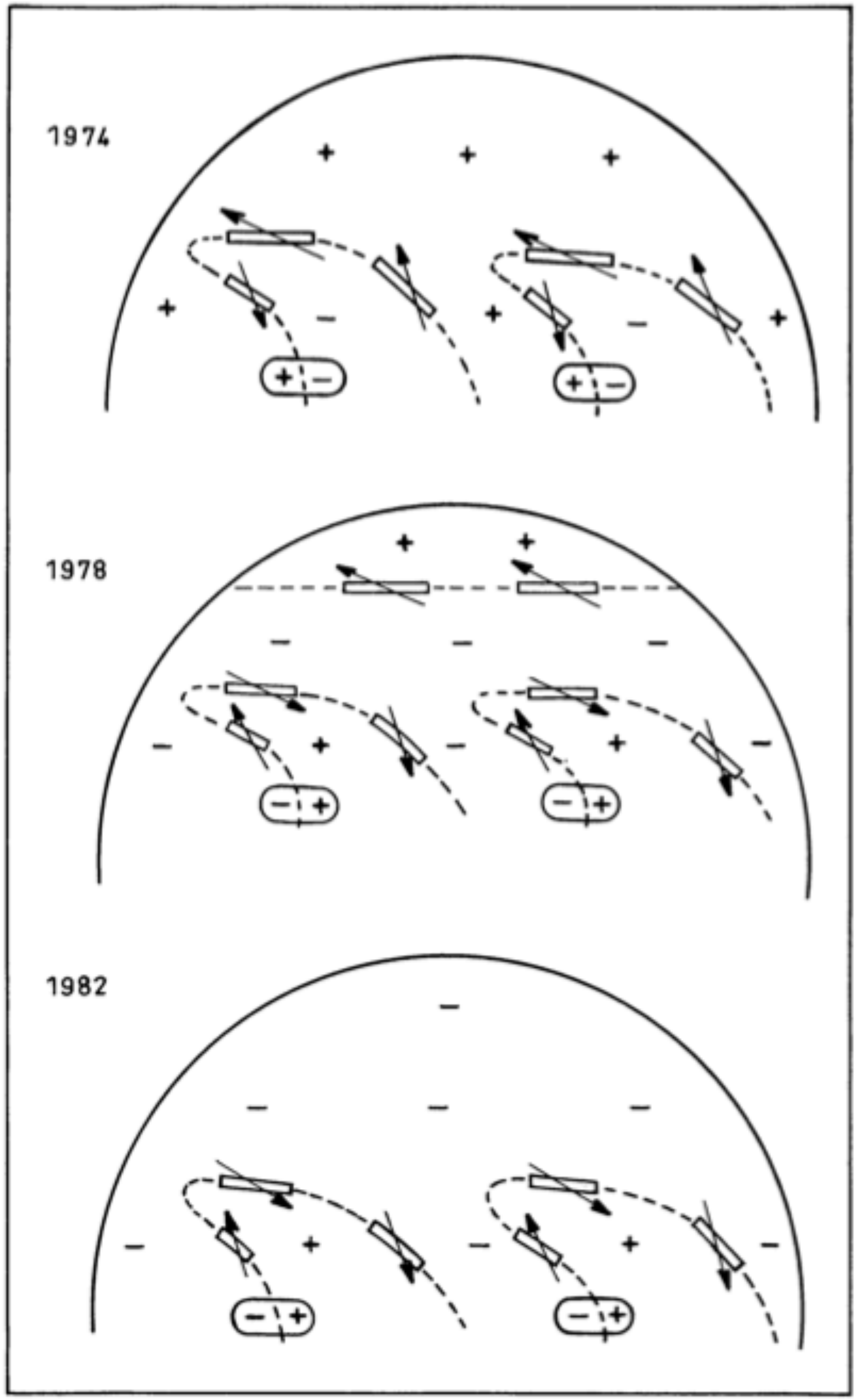

Leroy, Bommier, Sahal-Bréchot, 1984, A&A, 131, 33

Sac Peak

3rd GENERATION HANLE EFFECT OBSERVATIONS

field strength | inclination

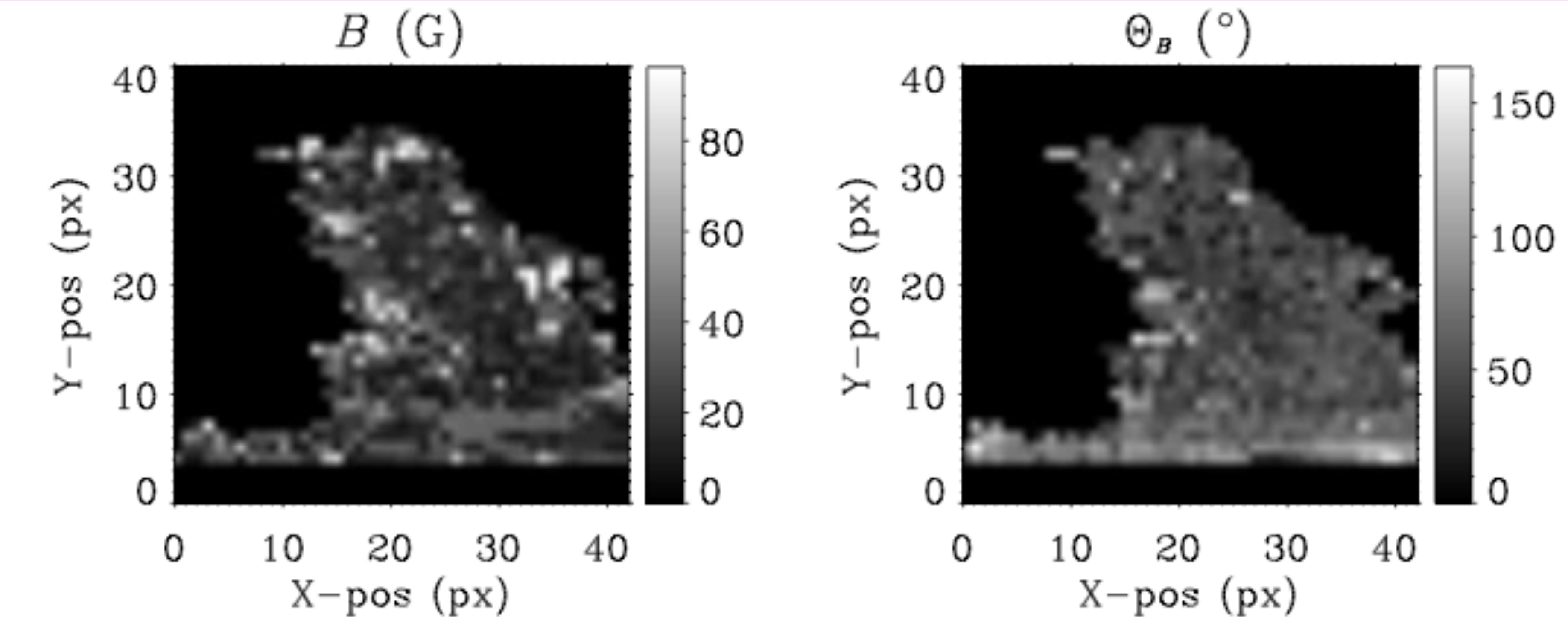

PCA inversion

Casini, Bevilacqua, Lopez Ariste, 2005, ApJ, 622, 1265

THEMIS telescope

3rd GENERATION HANLE EFFECT OBSERVATIONS

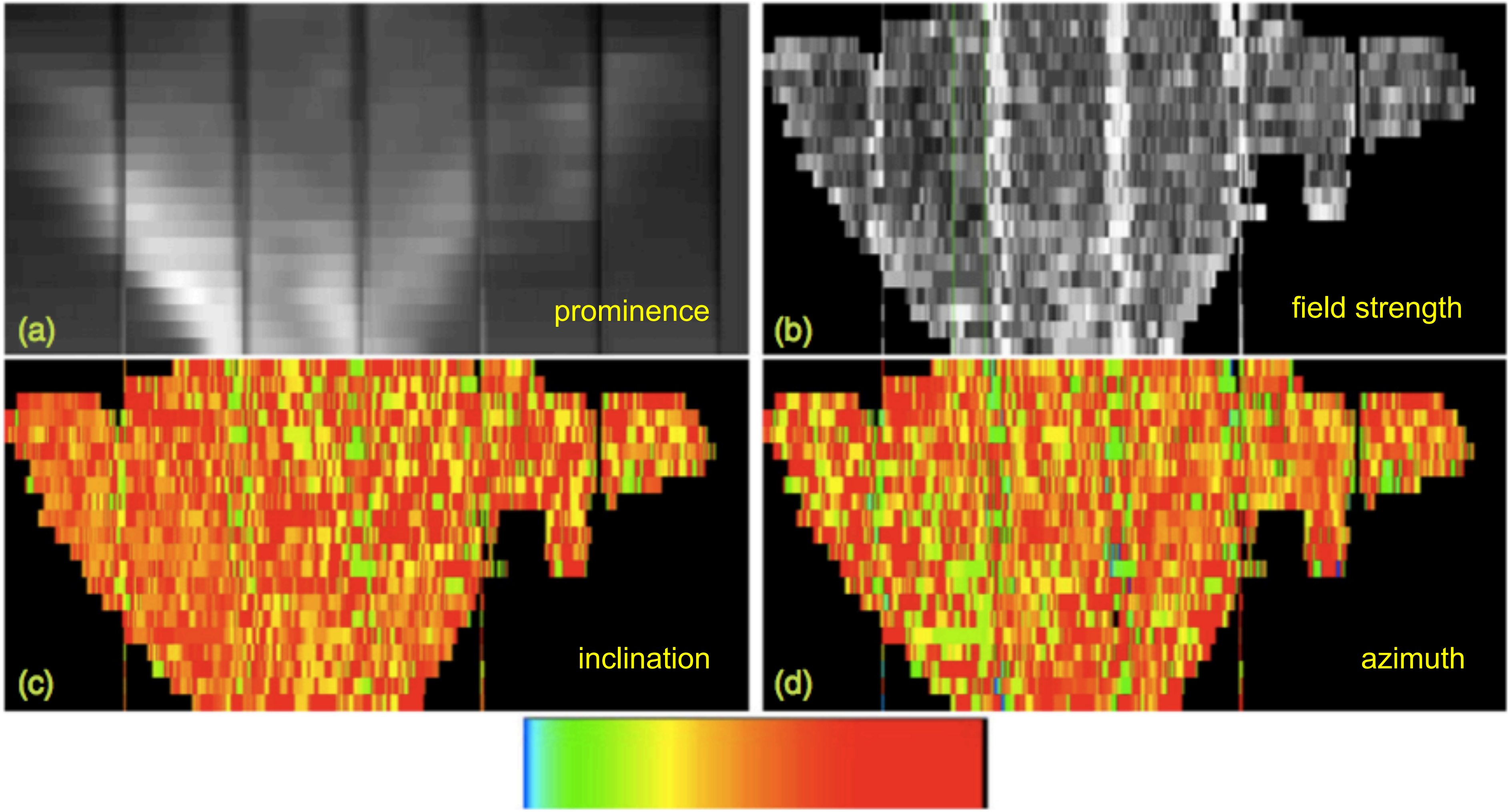

PCA inversion

Schmieder, Kucera, Khniznik, Luna, Lopez-Ariste, Toot, 2013, ApJ, 777, 108

THEMIS telescope

3rd GENERATION HANLE EFFECT OBSERVATIONS

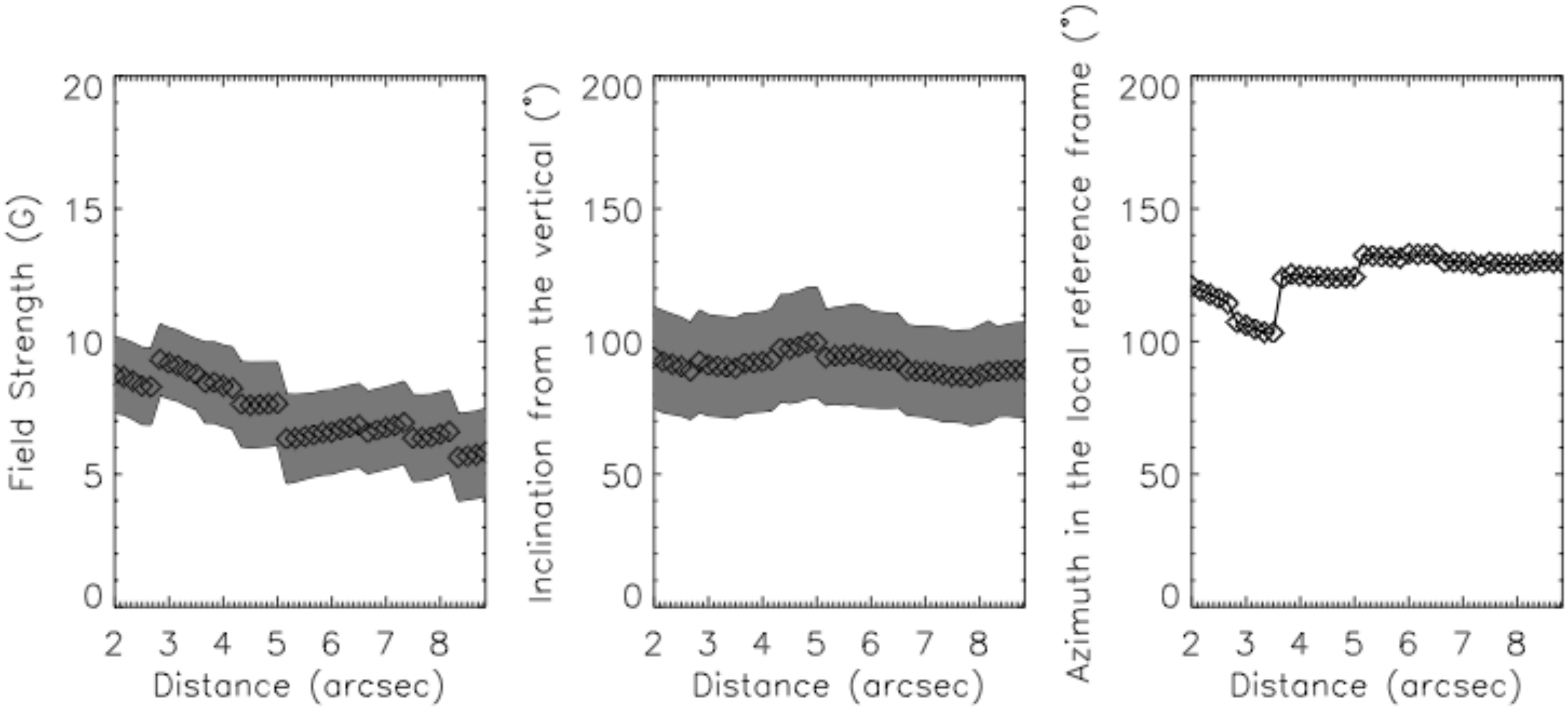

PCA inversion

Schmieder, Kucera, Khniznik, Luna, Lopez-Ariste, Toot, 2013, ApJ, 777, 108

THE HANLE EFFECT

line sensitivity

TABLE I

Domain of sensitivity to the Hanle effect of selected lines of astrophysical interest. B_{typ} is the 'typical' magnetic field defined by $\omega\tau = 1$ (cf. Section 2), and p_{lim} the maximum theoretical value of the polarization degree obtained for an infinite height above the solar limb

Spectrum	λ (Å)	Transition	B_{typ} (G)	P_{lim}
Fe XIV	5303	$3p\ ^2P_{3/2} \rightarrow 3p\ ^2P_{1/2}$	5×10^{-6}	0.43
C III	1909	$2s2p\ ^3P_1 \rightarrow 2s^2\ ^1S_0$	1.1×10^{-5}	1
He I	10 830	$2p\ ^3P_{2,1,0} \rightarrow 2s\ ^3S_1$	0.83	
He I (D_3)	5875	$3d\ ^3D_{3,2,1} \rightarrow 2p\ ^3P_{2,1,0}$	6	
He I (D_3)	major comp.	$3d\ ^3D_{3,2,1} \rightarrow 2p\ ^3P_{2,1}$	6	
He I (D_3)	minor comp.	$3d\ ^3D_1 \rightarrow 2p\ ^3P_0$	16	1
C IV	1548	$2p\ ^2P_{3/2} \rightarrow 2s\ ^2S_{1/2}$	22.5	0.43
N V	1239	$2p\ ^2P_{3/2} \rightarrow 2s\ ^2S_{1/2}$	28.7	0.43
O VI	1032	$2p\ ^2P_{3/2} \rightarrow 2s\ ^2S_{1/2}$	34.7	0.43
Si IV	1394	$3p\ ^2P_{3/2} \rightarrow 3s\ ^2S_{1/2}$	78.2	0.43
Si III	1206	$3s3p\ ^1P_1 \rightarrow 3s^2\ ^1S_0$	295.	1
Lα	1216		53.2	0.27
Lβ, Hα	1026, 6563		16	
Lγ, Hβ	992, 4861		7	

from Sahal-Bréchot, 1981, Space Science Rev. 29, 391